Far-infrared absorption of neutron-transmutation-doped germanium

H. F. Jang, G. Cripps*, and T. Timusk
Department of Physics, McMaster University, Hamilton, Ontario, Canada L8S 4M1
(Received 11 September 1989)

An investigation of the far-infrared absorption of compensated p-type Ge at a temperature of 3 K is presented. The absorption mechanism which is of interest is due to photon-induced hopping transitions of charge carriers between impurity centers. The samples were prepared by neutron transmutation doping. Samples with carrier concentrations $(N_a - N_d)$ ranging from 2.3×10^{15} to 2.6×10^{16} cm^{-3} show a broad maximum peaked at a frequency between 10 and 24 cm^{-1}. The absorption and the frequency of its maximum increase asymptotically with respect to time due to the evolution of the Ga-impurity concentration. It is found that at low frequencies the absorption coefficient is proportional to frequency. The overall behavior of the absorption spectra is found to be consistent with a theory based on the localized-pair model but a theoretically predicted sharp peak at 20.4 cm^{-1} on the absorption curve has not been observed in the experimental absorption spectra.

I. INTRODUCTION

Investigations of the far-infrared (FIR) absorption in compensated germanium and silicon doped with shallow impurities are of considerable interest since they provide information about the interaction between impurity centers, in addition to an understanding of the nature of disordered systems. Theoretical work on the low-temperature FIR absorption of lightly doped n-type materials with a low-compensation ratio ($K < 0.2$) was first proposed by Blinowski and Mycielski.[1] Their model is based on the localized-pair model, where the absorption is due to photon-induced hopping transitions of charge carriers in pairs of neutral and ionized donors situated near an ionized acceptor. Their theory has shown some agreement with the absorption measurements reported by Milward *et al.* for n-type Si,[2] and Demeshina *et al.* for n-type Ge.[3]

However, the situation for p-type materials is not well established compared to n-type materials. There have been no experiments done on p-type Si and few absorption measurements have been made on p-type Ge. The absorption in Ge:Ga was measured in the 16–50 cm^{-1} range by Smith *et al.*[4] and Zwerdling *et al.*;[5] however, their measurements are only able to determine the absorption coefficients to an order of magnitude. The absorption in Ge:In was reported for the region extending from 10 to 100 cm^{-1} by Nakagawa *et al.*[6] Most recently, a study of the absorption of submillimeter and millimeter radiation (3–15 cm^{-1}) on neutron-transmutation doped (NTD) compensated p-type Ge was performed by Vavilov *et al.*[7]

A comparison between the p-type experimental spectra and the n-type theory of Blinowski and Mycielski shows that they differ appreciably. To account for such differences, Kaczmarek *et al.* developed an absorption theory for p-type semiconductors.[8] They use, essentially, the same theoretical model as Blinowski and Mycielski for the n-type case, except that they use a different envelope function to describe the isolated-acceptor ground state. However, the existing experimental data cannot be used to justify the theory. Clearly, more work is needed in order to achieve a better understanding of photon-induced hopping absorption for p-type materials.

In this paper, the results of far-infrared absorption experiments on compensated NTD Ge at a temperature of 3 K will be presented. The purpose of this research is to investigate the properties of far-infrared absorptions for p-type Ge in detail and compare them to existing theories.

NTD Ge is chosen for such studies because of the high quality of this doping technique.[9] The investigation of far-infrared absorption in NTD Ge is of considerable interest since these materials are widely used as sensitive bolometers for the detection of FIR radiation at low temperatures.[10] Moreover, the unique properties of NTD Ge provide the opportunity to study two different dependences of the absorption spectra. First, the dependence of a sample's absorption on impurity concentration with the same degree of compensation can be studied. This is possible for NTD Ge samples because the concentration is varied by the irradiation time and the compensation is fixed by the nuclear reaction. Seven samples with carrier concentrations $(N_a - N_d)$ ranging from 1.3 to 26×10^{15} cm^{-3} were prepared for this experiment. The impurity concentrations of these samples are on the insulator side of the Mott transition.[11,12] Nevertheless, these

samples cover the important range of impurity concentrations in which the results can be compared with the present absorption theory. Second, the dependence of absorption for samples with different majority impurity concentrations, but with the same minority impurity concentration, can be studied. This is possible by doing a time-dependent absorption experiment after the irradiation, as will be discussed.

The plan of this paper is as follows. In Sec. II the necessary background theory for understanding this absorption process is briefly discussed. The preparation of NTD Ge samples, the FIR transmission experiment, and the derivation of the optical parameters from the transmission spectra are presented in Sec. III. Section IV presents results and discussion of the far-infrared absorption experiments: the changes in the absorption spectra due to the change in the impurity concentration with a fixed compensation ratio, and the change of majority impurity concentration with fixed minority concentration are discussed. The general characteristics of the spectra will be compared with the existing theory based on the localized-pair model and particularly the spectra predicted by Kaczmarek *et al.*[8] for p-type Ge. The spectra are also compared to the experimental work done by Vavilov *et al.*[7] on NTD Ge, and by Milward *et al.*[2] on n-type Si. Section V contains our conclusions along with a summary of the results.

II. THEORY OF FIR ABSORPTION

Theoretical investigations of the absorption at low temperatures in the far-infrared for n-type compensated Ge and Si were carried out by Blinowski and Mycielski,[1] Banaszkiewicz,[13] and most recently by Baranowskii and Uzakov.[14] At low temperatures, in a compensated n-type semiconductor, all the acceptors, N_a, will be ionized. Therefore, there are an equal number of ionized donors and acceptors, and $(N_d - N_a)$ donors will remain neutral. If the impurity concentration is low, then it is possible to treat the photon absorption as the result of zero-phonon electron transitions in pairs of ionized and neutral donors. This process, called direct absorption, was first proposed by Tanaka and Fan.[15]

The two lowest electron states of the two-center Hamiltonian were obtained by Miller and Abrahams:[16]

$$\varepsilon^{\pm} = (\varphi_1 + \varphi_2)/2 \pm \Gamma/2, \tag{1}$$

where φ_1 and φ_2 are the ground-state energies of the site 1 and site 2 impurities. The energy separation (Γ) denotes separation in energy of these two lowest states with some approximations, and is given by[14]

$$\Gamma = (\Omega^2 + 4I^2)^{1/2}, \tag{2}$$

where Ω is the difference between the Coulomb potential energies of the two centers of the donor pair. In general Ω is created by all the surrounding charges. I is the energy overlap integral which is usually anisotropic. Under the influence of FIR radiation, the electron will be excited from one level to the other. The pairs of donors for which $\Omega \ll 2I$ are called homopolar pairs; whereas, when $\Omega \gg 2I$, they are called polar pairs.

The absorption coefficient $\alpha(\omega)$ of such a system at a temperature T can be found:[14]

$$\alpha(\omega) = \frac{16\pi^3 e^2}{3c\hbar\kappa^{1/3}}\left[1 - \exp\left(-\frac{\hbar\omega}{kT}\right)\right] \times \int_{r_\omega}^{\infty}\left(\frac{r^4 I^2(r)}{[\hbar^2\omega^2 - 4I^2(r)]}\frac{1}{2} \times F([\hbar^2\omega^2 - 4I^2(r)]^{1/2}, r)\right)dr, \tag{3}$$

where c is the speed of light and the distribution function $F(\Omega, r)$ is defined such that $4\pi r^2 F(\Omega, r)dr\,d\Omega$ is the probability of finding, in a unit volume, a pair consisting of an ionized and neutral donor separated by a distance within the interval $(r,\ r + dr)$ and with a difference in Coulomb energies within the interval $(\Omega, \Omega + d\Omega)$. The angular average of I, $I^2(r) = \langle I^2 \rangle$, is used in this equation. The quantity r_ω is found from the condition $2I(r_\omega) = \hbar\omega$. In the case of hydrogenlike centers such as the donors in Ge or Si, $I(r)$ can be expressed as[16]

$$I(r) = I_0(r/a)^{3/4}\exp(-r/a), \tag{4}$$

which is valid when $r \gg a$, where a is the localization radius and I_0 is an energy of the order of the donor state energy. Then, r_ω is given by the equation,

$$\frac{r_\omega}{a} = \ln\frac{2I_0(r_\omega/a)^{3/4}}{\hbar\omega}. \tag{5}$$

For $r \approx r_\omega$, the energy overlap integral $I(r)$ is large and the denominator in the integral, $[\hbar^2\omega^2 - 4I^2(r)]^{1/2}$, remains small. It is clear from Eq.(3) that if $F(\Omega, r)$ is a slowly varying function compared with the exponential function then the main contribution to the absorption at a frequency ω is due to the pairs with an internal distance of the order of r_ω. That is, homopolar pairs will contribute significantly to the absorption process.

In order to calculate the absorption coefficient, the function $F(\Omega, r)$ needs to be known. However, there is no analytical theory to find $F(\Omega, r)$ even if quantum effects are ignored. Baranovskii and Uzakov[14] calculated $F(\Omega, r)$ by using a Monte Carlo technique to model an impurity band within the classical impurity band (CIB) model.[12,17] Their results make it possible to calculate, at fairly low frequencies, the absorption coefficient for materials within a wide range of compensation, K, from 0.1 to 0.9.

Within the CIB model, in the case of small compensation ($K < 0.2$),[1] it can be assumed that all donors except the ones nearest to an acceptor are neutral, and that the potential is due to the Coulomb potential of this ionized acceptor. The dipole potentials of other ionized acceptors and ionized donor pairs present in the materials are ignored. Let r_1 and r_2 be the distances from the ionized acceptor to the ionized and neutral donors,

respectively. The distance r between the sites in the pair and the Coulomb energy are given by

$$r = (r_1^2 + r_2^2 - 2r_1 r_2 \cos\theta)^{1/2}, \tag{6}$$

$$\Omega = \frac{e^2}{\kappa}\left(\frac{1}{r_1} - \frac{1}{r_2}\right), \tag{7}$$

where θ is the angle between the directions of r_1 and r_2. Under such an assumption, an analytic formula for $F(\Omega, r)$ is given by[18]

$$4\pi r^2 F(\Omega, r) = N_a N_d^2 \int dr_1 \int dr_2 \exp(-\tfrac{4}{3}\pi r_1^3 N_d)\delta[r - (r_1^2 + r_2^2 - 2r_1 r_2\cos\theta)^{1/2}]\delta\left(\Omega - \tfrac{e^2}{\kappa r_1} + \tfrac{e^2}{\kappa r_2}\right). \tag{8}$$

Integrating with respect to the angle θ and also with respect to the modulus r_2, the expression for $F(\Omega, r)$ becomes

$$F(\Omega, r) = \frac{2\pi}{r}\frac{N_d^2 N_a \kappa}{e^2}\int_{R_1}^{R_2} \frac{r_1^4 \exp\left(-\frac{4}{3}\pi r_1^3 N_d\right)}{\left(1 - \frac{\kappa}{e^2}\Omega r_1\right)^3} dr_1, \tag{9}$$

where

$$R_1 = \frac{r}{2} + \frac{e^2}{\kappa\Omega} - \frac{1}{2}\left[r^2 + \left(\frac{2e^2}{\kappa\Omega}\right)^2\right]^{1/2}, \tag{10}$$

$$R_2 = \min\left\{\frac{1}{2}\left(r^2 + \frac{4e^2 r}{\kappa\Omega}\right)^{1/2} - \frac{r}{2}, r_\mu\right\} \tag{11}$$

and

$$r_\mu = \frac{e^2}{\kappa\mu}, \tag{12}$$

where $\mu = 0.61\varepsilon_d$ is the Fermi energy for a low degree of compensation. r_μ takes into account the fact that the donor nearest to the acceptor will not be ionized if its distance from the acceptor exceeds r_μ.

The function $F(\Omega, r)$ described above is proportional to N_a, and the integral depends only on N_d. Hence, in the case of a low degree of compensation ($K < 0.2$), it follows from Eq.(3) that the (α/K) spectra would be the same for a given value of N_d and the shape of the absorption curve does not depend on the concentration of the minority impurity.

At this point it would be useful to obtain expressions for the absorption for the low- and high-frequency limits within this localized model. It can be shown that at the limit of low frequencies, $\hbar\omega \ll er_\omega E_N$, where $E_N = eN_d^{2/3}/\kappa$ is the characteristic scale; the absorption coefficient $\alpha(\omega)$ can be obtained as[17]

$$\alpha(\omega) = \frac{4\pi^3}{6c} a\omega r_\omega^3 N_d^{4/3} K f(K), \tag{13}$$

where $f(K)$ is a function of compensation. In the case of low compensation ($K < 0.2$) [i.e., if $F(\Omega, r)$ described in Eqs. (9)–(12) is used], $f(K)$ is independent of K. Equation (13) is derived for compact pairs with $a \ll r_\omega \ll r_d$ and $\Omega \approx 0$. The dipole-dipole interaction, which can give an extra factor depending on the frequency logarithmically,[17] is ignored in Eq. (13).

It has been predicted by Efros and Shklovskii[19] that the density of states falls off in the vicinity of the Fermi level and this is known as the Coulomb gap. The origin of such behavior is related to the long-range Coulomb interaction between charges. For the case of an intermediate compensation, the width of the Coulomb gap (Δ) is of order of the impurity band. The absorption at very low frequencies, $\hbar\omega << e^2/\kappa r_\omega << \Delta$, is obtained independently by Shklovskii and Efros,[20] and Davies *et al.*:[21]

$$\alpha(\omega) \propto \frac{\omega}{r_\omega} \propto \frac{\omega}{\ln(2I_0/\hbar\omega)}, \tag{14}$$

where $r_\omega \propto \ln(2I_0/\hbar\omega)$ is assumed [see Eq. (5)]. Hence, the dependence of absorption on frequency in Eq. (14) is stronger than linear.

In the limit of high frequencies, $\hbar\omega \gg er_\omega E_N$, one has to take into account that $F(\Omega, r)$ decreases steeply as Ω increases for $\Omega \gg er_\omega E_N$. Then the main contribution to the integral in Eq. (3) comes from a narrow interval near $r \approx r_\omega$, where $\Omega \approx er_\omega E_N \ll \hbar\omega$. In this case, the function $r^4 F(\Omega, r)$ in the integral is assumed constant for $\Omega \leq er_\omega E_N$ and zero otherwise. Then the absorption coefficient $\alpha(\omega)$ can be obtained:[17]

$$\alpha(\omega) \approx \frac{4\pi^3 e^2}{3c\hbar\kappa} a r_\omega^4 N_d^2 K f(K). \tag{15}$$

At low frequencies, $\hbar\omega < er_\omega E_N$, only pairs with $\Omega \leq \hbar\omega$ will participate in the absorption. Therefore, the absorption increases with increasing frequency. However, at high frequencies, $\hbar\omega > er_\omega E_N$, the contribution is from $\Omega < er_\omega E_N$, where r_ω decreases with increasing frequency. It follows from the above analysis that $\alpha(\omega)$ has a maximum[17] at

$$\hbar\omega_{\max} \approx er_\omega E_N = \frac{e^2 N_d^{2/3}}{\kappa} r_\omega. \tag{16}$$

It is known that the low-frequency ac impurity conduction at low temperatures in p-type materials is similar to that in n-type materials. However, previous experimental data showing the far-infrared spectra of p-type Ge differ appreciably from those of n-type Ge. The differences are as follows.[8] (i) The maximum value of the absorption

coefficient of p-type Ge is much higher than that for n-type Ge, (ii) the maximum of the absorption coefficient for p-type Ge occurs at higher frequencies than that of n-type Ge, and (iii) the dependence of the absorption coefficient on frequency for p-type Ge is not as strong as that of n-type materials.

In order to explain these differences, Kaczmarek and Gortel[8] used the envelope functions introduced by Schechter[22] to describe the isolated-acceptor ground state rather than using the well-known hydrogenlike envelope function. The latter picture is qualitatively similar to that for n-type materials in which the donor ground state is described by the hydrogenlike functions with an anisotropic exponent. The basic difference between the two pictures is that the Schechter function in p-type materials will give the four lowest two-center states formed by the ground states of the two impurities;[23] while there are only two in the latter case. All of these four states have different energies and should be taken into account when calculating the low-temperature absorption coefficient in the infrared.

The reason that the use of the Schechter envelope functions is essential in calculating the absorption coefficients for p-type materials has been pointed out by Gortel *et al.*[24] It can be shown that if the dominant contribution to the absorption is due to the polar pairs, then the results from a hydrogenlike approximation would agree qualitatively with the results from the model based on the Schechter envelope functions. In fact, this conclusion explains the similarities of ac impurity conductivity in both n- and p-type materials because the dominant contribution to the hopping conductivity is from those polar pairs. However, for the contribution from the homopolar pairs[24] the results of these two models are different both qualitatively and quantitatively. It was stated earlier that the homopolar pairs give an important contribution to the far-infrared absorption processes. Therefore, the use of the hydrogenlike approximation is not appropriate here.

It is found that by using the Schechter envelope function, the photon-induced transition rate of a carrier is dominated by two terms.[24] The first term has a form analogous to that of the n-type material. This term is proportional to the square of the overlap energy integral, which for a pair with a given separation is larger for the p-type than for the n-type material. The second term, which is absent in the hydrogenlike approximation, is even larger than the first term for some directions. Therefore, the much larger absorption in the p-type material is expected when the Schechter envelope function is used. Also, the larger value of the resonance energy can also explain the shift in the maximum of the absorption towards higher frequencies.

The theory also predicts a sharp absorption peak at 20.4 cm^{-1}. Its position does not depend on the compensation or on the concentration of acceptors. The shape and relative height of the peak is temperature independent.[8] The presence of this peak is a direct result of the nonmonotonic behavior of the overlap energy integral $\langle I_1^2 \rangle$ as a function of the pair separation which is a consequence of the d-like parts in the Schechter envelope functions for isolated acceptors. Because of the slow variation of $\langle I_1^2 \rangle$ in the vicinity of its maximum value, a large number of pairs can absorb radiation with the energy $\hbar\omega = 2(\langle I_1^2 \rangle_{max})^{1/2}$. Therefore, the position of this sharp peak is determined by $\hbar\omega = 2(\langle I_1^2 \rangle_{max})^{1/2}$.

III. EXPERIMENT

A. Principle of NTD Ge

The Ge samples were irradiated with thermal neutrons at the McMaster Nuclear Reactor. Some of the five naturally occurring stable isotopes, ^{70}Ge, ^{72}Ge, ^{73}Ge, ^{74}Ge, and ^{76}Ge, capture neutrons and become radioactive and subsequently decay into different chemical elements which are acceptor or donor impurities in Ge. Three Ge isotopes, ^{70}Ge, ^{74}Ge, and ^{76}Ge participate in the doping process. The nuclear reactions of interest are[10]

$$^{70}_{32}\mathrm{Ge}(\mathrm{n},\gamma)^{71}_{32}\mathrm{Ge} \xrightarrow{T_{1/2}=11.2\ \mathrm{d}} {}^{71}\mathrm{Ga}(\beta^- \text{capture}), \quad (17)$$

$$^{74}_{32}\mathrm{Ge}(\mathrm{n},\gamma)^{75}_{32}\mathrm{Ge} \xrightarrow{T_{1/2}=82.8\ \mathrm{m}} {}^{75}\mathrm{As}(\beta^- \text{ decay}), \quad (18)$$

$$^{76}_{32}\mathrm{Ge}(\mathrm{n},\gamma)^{77}_{32}\mathrm{Ge} \xrightarrow{T_{1/2}=11.3\ \mathrm{h}} {}^{77}\mathrm{As}(\beta^- \text{ decay})$$

$$\xrightarrow{T_{1/2}=38.8\ \mathrm{h}} {}^{77}\mathrm{Se}(\beta^- \text{ decay}). \quad (19)$$

The natural abundance, thermal neutron absorption cross sections, and half-lives of the relevant isotopes of Ge are listed in Ref. 10. After all the decay processes are exhausted, the ratio of the concentrations of the different dopants, i.e., the compensation (K), will be fixed by the thermal neutron capture cross section and natural abundance of the dopant-producing isotopes. According to the experimental results of Osip'yan *et al.*,[25] which are based on time-dependent Hall measurements, the degree of compensation $K = N_a/N_d$ for NTD Ge is ≈ 0.27. These results are in fair agreement with the theoretical results obtained using the nuclear reaction data.[26] This doping method allows us to investigate the absorption change of Ge samples due to the change of the impurity concentration with fixed compensation.

As a result of different decay half-lives, different impurities are formed at different rates. As, which is the dominant donor impurity, reaches its saturation value within a day after irradiation due to the short decay half-life (82.8 m) of ^{74}Ge. The Se donors also reach 80% of their saturated value about 5 days after irradiation. However, because of the longer decay half-life (11.2 d) of ^{71}Ge, the concentration of the acceptor impurity reaches the value of N_d only after a time $t = t_{(K=1)}$ of the order of several days after the start of irradiation. The NTD Ge sample, which is n-type for $t < t_{(K=1)}$, will convert to p-type at $t = t_{(K=1)}$. For $t > t_{(K=1)}$ the degree of compensa-

tion will decrease with time and approach asymptotically to the steady-state value. These decay properties of NTD Ge allow us to investigate the change in absorption due to the change in the majority impurity concentration while keeping the minority impurity concentration constant. This is done by performing time-dependent absorption experiments after the donor impurities have reached their saturated value and the acceptors are still being formed.

The concentration, $N(t)$, of a particular impurity at time t after starting the irradiation can be calculated using the following expressions:

$$N(t) = \begin{cases} N_0\left(\frac{1}{t_r}\left\{t - \frac{\tau}{\ln 2}\left[1 - \exp\left(-\frac{\ln 2}{\tau}t\right)\right]\right\}\right), & t \le t_r \quad (20) \\ N_0\left\{1 - \frac{\tau}{(\ln 2)t_r}\left[\exp\left(-\frac{(\ln 2)(t-t_r)}{\tau}\right) - \exp\left(-\frac{\ln 2}{\tau}t\right)\right]\right\}, & t \ge t_r \quad (21) \end{cases}$$

where N_0 is the saturated concentration of an impurity long after irradiation, t_r is the time of neutron irradiation, and τ is the decay half-life of an unstable isotope.

B. Sample preparation

The starting materials for the NTD Ge samples were single-crystal low impurity n-type Ge wafers with $(N_d - N_a) < 10^{12}$ cm^{-3} with thicknesses of about 0.05 cm. These wafers were cut into pieces 1 x 1 cm^2 in size. They were then irradiated with thermal neutrons at approximately 35 °C. The thermal neutron flux at the position of irradiation was $\approx 1.4 \times 10^{13}$ cm^{-2}sec^{-1} (Ref. 27) with a ratio of thermal neutrons to neutrons with energy greater than 0.5 eV of approximately 40 : 1.

Seven samples, 1–7, were irradiated for different time intervals varying from 1 to 20 h. The production of various impurities is proportional to the neutron fluence. The concentrations of the Ga impurities in these samples are estimated[27] from the known reaction data as shown in Table I. These samples, all of which have the same compensation ratio long after the irradiation, were used for absorption experiments which investigated the change in absorption with changing concentration.

Except for the sample which is used for the time-dependent absorption experiment, samples are kept for more than 3 months after irradiation before they are used for the absorption experiments. The samples are thinned using 600-grit SiC paper. Opposite surfaces of the samples are made parallel. Both surfaces are mechanically polished using 6 μm and then 1 μm diamond grit paste. The thickness of the samples was determined using a micrometer with an uncertainty of ± 0.005 mm (see Table I).

Radiation damage of the samples was removed by thermally annealing at 400 °C for 6 hours in a pure argon atmosphere.[10] All samples were placed into the furnace at a temperature below 100°C and were taken out only after the furnace had cooled to room temperature.

The square samples were characterized by Hall-effect measurements using the usual van der Pauw configuration[28] with magnetic fields of approximately 1 KG. Ohmic contacts were made by alloying indium to the four corners of the samples. This was done by heating with a low powered soldering gun. The room-temperature transport properties of samples 1–7 are shown in Table II. The carrier concentrations, $n = (N_a - N_d)$, and mobility, μ, were calculated from $n = r_H/R_H e$, and $\mu = R_H/r_H\rho$.[29] The Hall coefficient, R_H, and resistivity, ρ, were obtained from the measurements. The Hall factor, r_H, in the weak-field limit was found experimentally to be ≈ 1.8 by Morin.[30] The present data is in agreement with the existing transport properties of p-type Ge.[29] The results of the time-dependent electrical measurement which will be discussed later, show that the compensation of these samples is 0.286. Hence, the acceptor concentrations, N_a, for these samples are calculated using this value. A comparison of these values of N_a with the Ga concentrations estimated from the nuclear reactions in Table I shows good agreement.

TABLE I. Physical data for NTD Ge samples.

Sample	Irradiation time (h)	Fluence (10^{17} cm^{-2})	Ga concentration (10^{15} cm^{-3})	Thickness (mm)
1	1	0.5	1.7	0.475
2	2	1.0	3.4	0.490
3	4	2.0	6.8	0.440
4	8	4.0	14	0.469
5	10	5.0	17	0.499
6	16	8.1	27	0.489
7	20	10	34	0.366

TABLE II. Hall measurement data for NTD Ge samples.

Sample	Resistivity (Ω cm)	Hole mobility (cm^2/V sec)	$(N_a - N_d)$ (10^{15} cm^{-3})	N_a (10^{15} cm^{-3})
1	2.53	1840	1.34	1.88
2	1.54	1740	2.32	3.25
3	0.823	1520	4.97	6.96
4	0.458	1370	9.92	13.9
5	0.335	1200	15.5	21.7
6	0.286	1150	19.1	26.7
7	0.223	1080	26.1	36.5

Sample 5 is used for the time-dependent absorption experiment. This sample was annealed 3 days after the start of the irradiation using the same procedure as described above. The annealing done at this early stage does not affect the quality of the sample as shown by its high Hall hole mobility. This is in agreement with previous results[31] which indicate that the formation of defects is mainly due to the radiation damage which can be removed by annealing.

C. The FIR transmission experiments

The transmission experiments in the far infrared are done using Fourier transform spectroscopy. A custom built polarizing interferometer with roof mirrors, a wire grid beam splitter, and a chopper frequency of 45 Hz was used. The light source was a fused quartz mercury-arc lamp. The FIR light passes through a polypropylene window into the cryostat.

A commercial cryostat [HD-3(L) Dewar, Infrared Laboratories, Inc., Tucson, AZ] with a composite-type Si bolometer with an operating temperature of approximately 1.25 K was used. Two moveable wheels were placed inside the cold working surface of the cryostat. One of them is used to hold different cold cut-off filters so that they can be changed during the experiment. The other is to hold the sample and the reference. The light that passes through the filter and sample is then collected by a parabolic cone which condenses the light onto the bolometer.

Two stages are involved in filtering the light. Before reaching the sample, the radiation passes through a cold filter (cutoff $\approx$ 250 cm^{-1}) made of thick black polyethylene melted to a piece of gray plastic from the lid of a Kodak film canister. Both excess sample heating and band-edge light were prevented from reaching the sample by using this filter. Second, the radiation passes through one of three cold low-pass filters located in the filter wheel before reaching the bolometer. These filters define the cut-off energy of the spectra. They are 0.125 in thick Pyrex glass, 0.08 in thick Fluorogold, and 0.0625 in thick quartz with cut-off frequencies of 30, 50, and 120 cm^{-1} respectively. A 0.25 in thick Pyrex warm filter, which is placed outside the cryostat, was also used in conjunction with the cold filters for spectra with a cut-off of about 15 cm^{-1}. The transmission spectra presented here are obtained by linking spectra with different cut-off filters. All spectra were taken with a resolution of approximately 0.8 cm^{-1}.

The samples are glued to the sample holder by applying a small spot of GE 7031 varnish at one corner of the sample. The sample is placed over a 5 mm diameter opening in the sample holder. An opening with the same diameter as in the sample holder is used as a reference. The temperature of the sample is monitored using a 100-Ω Allen Bradley resistor placed in thermal contact with the sample. All spectra were taken with the sample temperature at about 3 K.

D. Derivation of the optical parameters

The transmittance of a material is determined by its index of refraction, $N = n + ik$. This index, in general, must be complex to account for the absorption within the material. The raw transmittance spectra show strong Fabry-Perot fringes which have to be removed. Following the work of Randall and Rawcliffe,[32] the external transmission $T(\nu)$ of a parallel flat-surfaced sample with thickness d, at the wave number ν, can be expressed as follows:

$$T(\nu) = \tau(\nu)\left(1 + 2\sum_{l=1}^{\infty}\rho^l \cos(l\theta)\right). \tag{22}$$

A more familiar form is

$$T(\nu) = \tau(\nu)\frac{(1-\rho^2)}{(1+\rho^2-2\rho\cos\theta)}. \tag{23}$$

In these expressions,

$$\tau(\nu) = |4N/(N+1)^2|^2 \exp(-\alpha d\cos\beta)/(1-\rho^2), \tag{24}$$

$$\tau(\nu) = 16(n^2+k^2)\exp(-\alpha d\cos\beta)/\{[(n+1)^2+k^2]^2(1-\rho^2)\}, \tag{25}$$

$$\rho = [(n-1)^2 + k^2]\exp(-\alpha d\cos\beta)/[(n+1)^2 + k^2], \tag{26}$$

$$\theta = 4\pi n\, d\nu\cos\beta + \delta$$
$$= 4\pi n\, d\nu\cos\beta + \tan^{-1}[2k/(n^2 + k^2 - 1)], \tag{27}$$

$$\alpha = 4\pi k\nu, \tag{28}$$

where α is the absorption coefficient, τ is the average transmittance if there are no fringes, δ is the phase shift in reflectance at the surface caused by the imaginary part of the refractive index, ρ is the fraction of the energy which survives two reflections and two transmittances through the body of the sample, and β is the angle of incidence of the radiation. In these experiments β is assumed to be zero.

In order to evaluate the absorption coefficient of a sample, the real part of the refractive index n will first be found from the interference fringes of the transmission spectrum. Since δ is small in these samples and can be neglected as a first approximation, it follows from Eqs. (22) or (23) that the transmittance maximum occurs at

$$\theta = 4\pi n\, d\nu = 2\pi m \tag{29}$$

where m is an integer that is of the order of the interference maximum at frequency ν. Since the transmittance is measured down to 4 or 5 cm^{-1}, the value for m is known and the refractive index can be obtained from the maximum of the transmission spectrum according to Eq. (30).

According to the treatment of Zwerdling and Theriault,[5] if α and n are essentially constant over the spectral range of one cycle of the interference, the absorption coefficients can be obtained from the average transmittance τ. It can be shown using Eq. (23) that τ can be obtained from the geometric mean of the maximum and minimum values.

However, since the resolution of the transmission spectra is chosen to be about 0.8 cm^{-1}, only the first signature of the fringes is significant in the interferogram. This implies that only the first cosine term of the series in Eq. (22) is important. That is, the observed transmission spectrum is given by

$$T(\nu) = \tau(\nu)[1 + 2C\rho\cos(\theta)], \tag{30}$$

where a parameter C is put in front of the cosine term because an apodization function[33] is used before an interferogram is Fourier transformed into a frequency spectrum. In this case, the average transmittance should be the average value of the maximum and minimum values at the frequency corresponding to the average of their frequencies.

The absorption coefficient α can be found from the following relationship which is derived from Eq. (25) with β set to zero:[5]

$$\alpha = \frac{1}{d}\ln\left\{\frac{(1-R)^2 A}{2\tau} + \left[\left(\frac{(1-R)^2 A}{2\tau}\right)^2 + R^2\right]^{1/2}\right\}, \tag{31}$$

where $A = (1 + k^2/n^2)$ and

$$R = \frac{(n-1)^2 + k^2}{(n+1)^2 + k^2} \tag{32}$$

is the reflectance at a single surface.

The process of finding the absorption coefficient, α, involves iteration of Eq. (31) by a computer one frequency at a time. Since k is small compared to n, it is first approximated as being equal to zero at the initial frequency. $\tau(\nu)$, as described above, is determined from the experimental transmission spectrum by taking the average value of the maximum and minimum values of the fringes observed in the spectrum at the frequency corresponding to the average of their frequencies. The value α is obtained from Eq. (31) and then a nonzero k is found. This process is repeated until the right- and left-hand sides of Eq. (31) are equal to within $\pm 0.000\,01\%$. This α will be used as the initial approximation for the next frequency $(\nu + \delta\nu)$.

Once the absorption spectrum is obtained using this procedure, the transmittance is calculated using Eq. (30). The original experimental spectrum will be compared with the calculated one with an appropriate choice of the adjustable parameter C in front of the cosine term. In general, at this stage, the constant parameter C is well fitted to a wide region of frequencies with no large discrepancies between the calculated and experimental transmission spectra. However, the above procedure will smooth a region with a sudden change in absorption or with sharp absorption peaks. In order to obtain a more detailed absorption spectrum at such regions, the experimental transmittance spectrum with the interference fringes will be fitted using Eq. (30) to find a new $\alpha(\nu)$. To a first-order approximation, the parameter C is assumed to be constant over the small frequency region which is being fitted. This parameter C is chosen such that the fringe structure is minimized in the resulting absorption spectrum. Then, this value of C combined with Eq. (30) is used to least-squares fit the experimental transmittance (with fringes) to find a new $\alpha(\nu)$. The value of $\alpha(\nu)$ derived from the average transmittance is used as a first guess. This procedure gives a more precise value of $\alpha(\nu)$ which ensures that sharp peaks are not missed. For instance, the sharp absorption lines result-

ing from the excited states of an impurity in the region above 40 cm^{-1} can be found in this manner.

IV. RESULTS AND DISCUSSION

A. Absorption spectra for NTD Ge

Figure 1 shows a typical transmission spectrum of a sample (sample 3) in the frequency region from 4 to 90 cm^{-1}. The interference fringes are due to the plane parallel surfaces of the samples. The real part of the refractive index, n, of these samples is found from these fringes using Eq. (30). The average refractive index of the samples for frequencies from 10 to 50 cm^{-1} is listed in Table III. It is found that the values for low impurity concentration samples (Nos. 1–4) are lower than the room-temperature values reported by Randall and Rawcliffe;[32] their measurements on intrinsic Ge samples with resistivities of 10 and 20 Ω cm give a value for n of about 4.005 in this frequency region. As shown in Table III, the refractive index of a sample increases as the impurity concentration of the sample increases; the refractive index increases from 3.88 for sample 1 to 4.04 for sample 7. The higher refractive index for doped Ge compared to intrinsic Ge at 4.2 K is also reported by Zwerdling and Theriault.[5]

There are two main absorption processes present in the transmission spectra: first, at lower frequencies (<50 cm^{-1}), the main absorption mechanism is due to far-infrared photon-induced hopping of a charge carrier between Ga impurity centers near an ionized donor. Second, the strong absorption region at high frequencies (>40 cm^{-1}) is associated with hole transitions from the ground state to excited states of the Ga impurity. A brief description of this latter absorption process will be given before a detailed discussion of the absorption due to the photon-induced hopping process is given.

The well-known excited states for the Ga impurities in Ge (Ref. 34) are labeled in Figs. 1 and 2. At low impurity concentrations (samples 1 and 2), it is possible to identify the excited states with the known Ga impurity excited states. However, as the impurity concentration increases, the broadening of the states makes such identification impossible. Figure 2 shows the absorption spectra from 30–80 cm^{-1} for samples 1–7 as obtained from the transmission spectra using the method described in Sec. III. At low concentrations, all impurities can be treated as noninteracting impurities which behave like isolated atoms. However, as the impurity concentration increases,

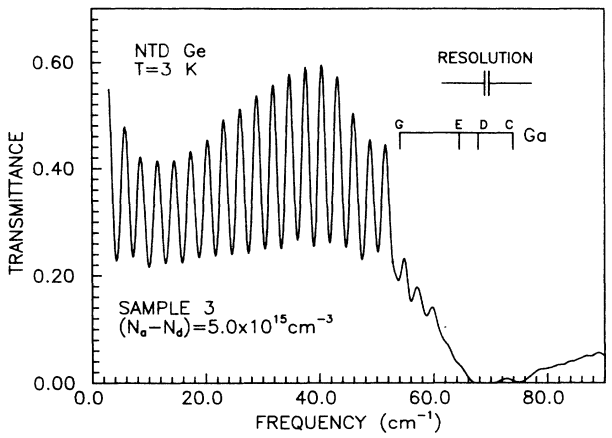

FIG. 1. Transmission spectra for NTD Ge sample 3 at a temperature of 3 K in the region from 0 to 90 cm^{-1}. The known Ga excited states are indicated.

it can be shown that the first effect on the isolated impurity is due to nearest-neighbor interactions.[35] The broadening of the lower edges of the sharp lines due to the increasing impurity concentration has been observed for both donors and acceptors in Si and GaAs.[35] It is concluded that the broadening is due to neutral impurity pairs for low impurity concentrations. Because the impurities are randomly distributed, the effect will first arise from pairs which are closer than average. Similar absorptions at the lower energy shoulders of excited states are also observed in these spectra as identified in Fig. 2. For instance, the absorption at the shoulder of the lowest state G, D_{G_1}, may be similar to the absorption due to the band states, $D_{1s}D_{2p_0}$, in P-doped Si. These shoulder absorptions are in fact due to excitations from the 1s to the $2p_0$ state of the same donor, but with another donor nearby in the ground state so that the energies of both ground and excited states are reduced. It is also observed that there is another absorption at energies lower than the $D_{1s}D_{2p_0}$ states.[35] This is attributed to the charge-transfer excitation forming D^+D^- with a considerable reduction in the energy of the excited state because of the Coulomb attraction. This excitation has been referred to as an exciton state located in the Hubbard band gap between D^- and D^+ states. The lowest absorption shoulder, D_{G_2}, may be due to the same charge-transfer

TABLE III. Refractive index of NTD Ge at T=3 K.

Sample	1	2	3	4	5	6	7
N_a (10^{15} cm^{-3})	1.88	3.25	6.96	13.9	21.7	26.7	36.5
n	3.88 ± 0.01	3.91 ± 0.01	3.94 ± 0.01	3.95 ± 0.01	4.00 ± 0.01	4.01 ± 0.01	4.04 ± 0.05

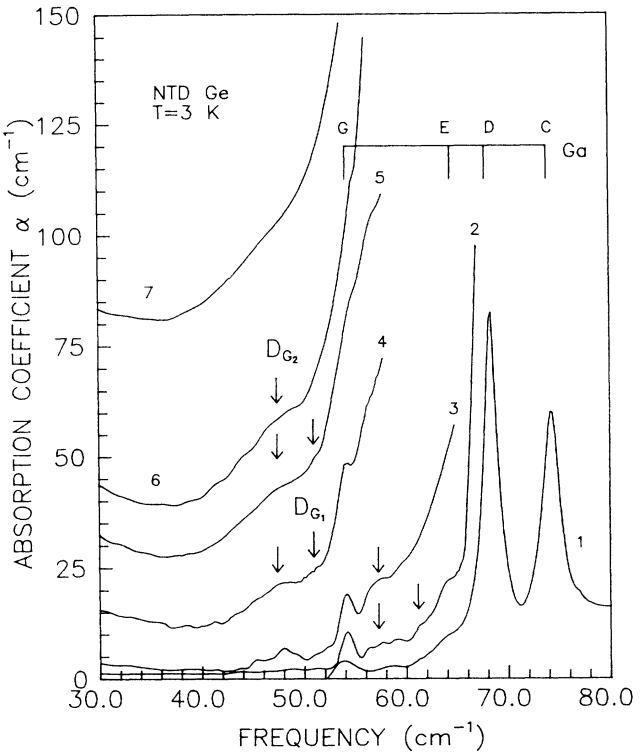

FIG. 2. Absorption spectra for samples 1–7 in the region from 30–80 cm^{-1}. The main absorption process in this region is due to the excitation of a neutral Ga impurity. The arrows indicate those absorptions due to neutral pairs with random separation.

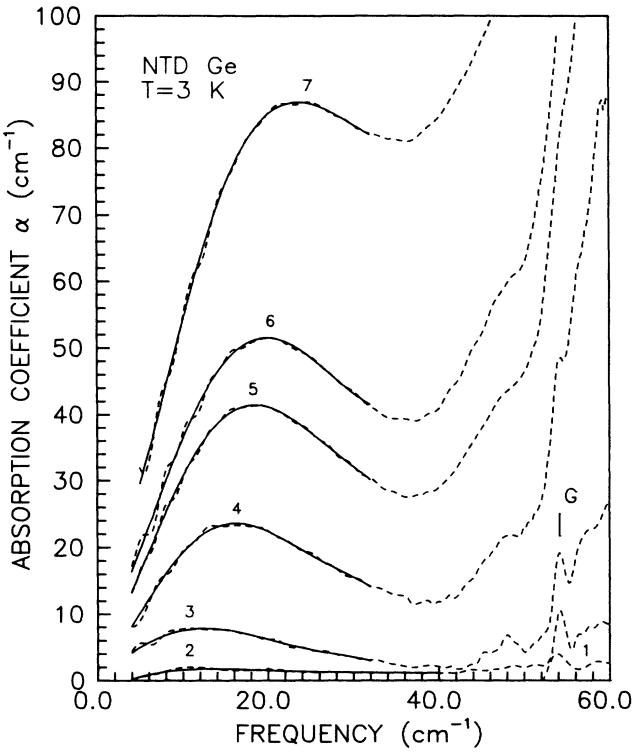

FIG. 3. Absorption spectra for samples 1–7 in the region from 0 to 60 cm^{-1}. The dashed lines are obtained from the transmission spectra. The solid lines are fits to a polynomial function for frequencies from 4 to 32 cm^{-1}. The main absorption process in this region is due to the photon-induced hopping of a charge carrier between acceptor pairs situated near an ionized donor.

excitation. This is not the same as the photon-induced hopping absorption discussed later because these pairs are neutral.

As the impurity concentration keeps increasing, the impurities will get closer to one another, thus forming triples and then clusters.[35] The effect of increasing the impurity concentration is to increase the number of larger clusters. The absorption edge is dominated by the localized states within random clusters of impurities with densities greater than the average. The cluster will give rise to the absorption at low energies. This effect is clearly demonstrated in these spectra. The absorption starts at lower frequencies as the concentration of the Ga impurity increases. It is noted that the absorption shoulder due to pair absorptions is not visible in the sample 7 spectrum.

Now, let us discuss the absorption due to photon-induced hopping. Figure 3 shows the absorption spectra from 4–60 cm^{-1} for samples 2–7. Broad absorptions are observed for samples 2–7. However, the absorption in this frequency region is negligible for sample 1. This indicates that the number of localized pairs is small at such low Ga concentration (1.9×10^{15} cm^{-3}). This is in agreement with the sharp lines observed for the excited states of Ga in this sample.

The absorption coefficient for all frequencies in this region increases as the samples' impurity concentration increases. The absorption coefficient at the maximum $[\alpha(\omega_{\max})]$ of the broad absorption curve increases from 2 cm^{-1} for sample 2 to 87 cm^{-1} for sample 7. The frequency of this maximum absorption ($\omega_{\max}$) also shifts to higher frequencies as the impurity concentration increases. The change is from 10 cm^{-1} for sample 2 to 23.8 cm^{-1} for sample 7. These results are listed in Table IV.

General properties of the absorption spectra versus net carrier concentration, $(N_a - N_d) = (1-K)N_a$, are plotted in Fig. 4. These data are least-squares fit to a power-law function $y = a(N_a - N_d)^n$. It is found that the power dependence for $\omega_{\max}$ and $\alpha(\omega_{\max})$ is $n = 0.37$ and 1.44, respectively. However, the absorption due to excitations of impurity centers has not been separated from the experimentally determined absorption spectra and hence, contributes to the absorption even at the frequency of the maximum. This is more serious for the high concentration samples because such absorption starts at lower frequencies. This is especially significant for sample 7; therefore, another best fit is done for the $\alpha(\omega_{\max})$

TABLE IV. ω_{max} and $\alpha(\omega_{max})$ of the absorptions.

Sample	1	2	3	4	5	6	7
$\omega_{max}(cm^{-1})$		10.0	12.0	16.2	18.6	20.2	23.6
$\alpha(\omega_{max})(cm^{-1})$	0	1.8	7.9	23.6	41.4	51.3	87.0

data without the data point from sample 7. It is found that $n = 1.31$ instead of 1.44 in this case. It is interesting to compare these results with the Blinowski and Mycielski theory for n-type materials described in Sec. II. Using Eqs. (3), (5), and (9)–(12), and appropriate parameters[14] for Si, it is found that ω_{max} is proportional to $N_d^{0.41}$ ($n = 0.41$) and that $\alpha(\omega_{max})$ is proportional to $N_d^{1.36}$ ($n = 1.36$) for n-type Si absorption spectra. These values are close to the experimental values for p-type NTD Ge samples presented here ($n = 0.37$ and 1.31).

According to Eq. (16), the frequencies of the maximum ω_{max} are predicted to be proportional to $N_a^{2/3} r_\omega$, where r_ω is the distance between the pairs which satisfies Eq. (5) at ω_{max}. Experimental results show that ω_{max} is proportional to $N_a^{0.37}$. Therefore, r_ω is proportional to $\approx N_a^{-0.3}$. That means that the value of r_ω at the maximum is roughly proportional to the average distance between majority impurities, $N_a^{-1/3}$, which is the characteristic scale of the system.

Least-squares fits to a linear function are done for the low-frequency region of the spectra as shown in Fig. 5. The best fit lines are extended to zero frequency. The

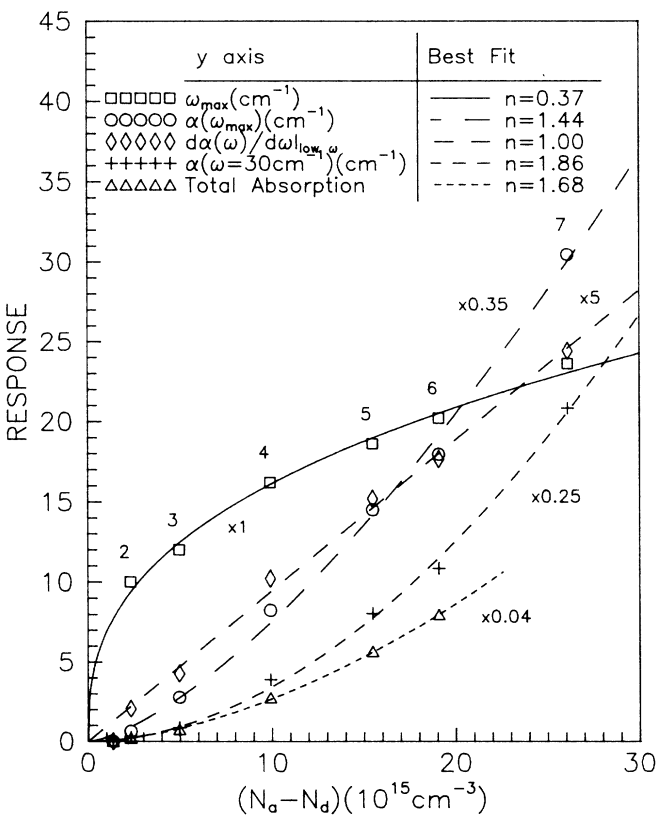

FIG. 4. General properties of the absorption spectra in Fig. 3 vs impurity concentration: (i) the frequency of maximum absorption (□), (ii) the absorption coefficient at the maximum (○), (iii) the slope of the spectra at low frequencies (◇), (iv) the absorption coefficient at 30 cm^{-1} (+), and (v) the estimated total absorption due to the photon-induced hopping process (△). The least-squares fits to the power-law function $y = a(N_a - N_d)^n$ are shown. The multiplication factor for the y-axis value for each curve is indicated.

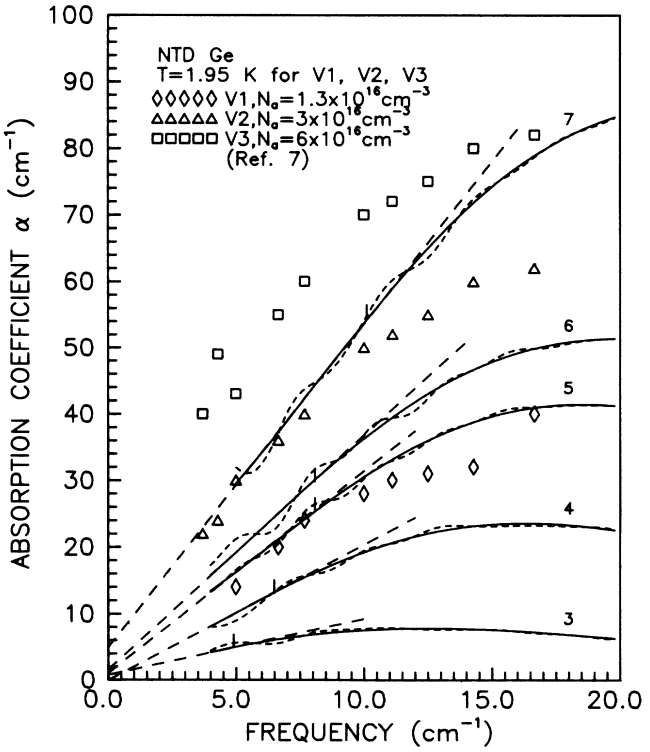

FIG. 5. The experimental absorption spectra $V1$, $V2$, and $V3$ obtained by Vavilov *et al.* The present results for samples 3–7 are shown together for comparison. Note that the longer dashed lines are the least-squares fits of linear functions at low frequencies. The "|" on the spectra denotes the upper limit of frequencies used for the linear fits. The values of the y intercepts for these linear fitted lines are consistent with the values obtained from the dc resistivity measurements (see text) except sample 3. The linear part of spectrum 3 probably occurs at lower frequencies (< 4 cm^{-1}) so that the extrapolated y intercept from the linear fit is too large in comparison with the value obtained from the dc measurement.

values of the y intercept are 0.75, -0.04, 1.0, 1.5, and 4.9 cm^{-1} for samples 3, 4, 5, 6, and 7, respectively. These values correspond to the absorption coefficients at zero frequency. It is noted that the absorption coefficient $\alpha(\omega)$ can be deduced from the conductivity $\sigma(\omega)$ as follows:[36]

$$\alpha(\omega) = \frac{4\pi\sigma(\omega)}{nc}, \tag{33}$$

where n is the refractive index and c is the speed of light. Substituting the value of $n = 4$ for Ge gives the relationship $\alpha(\omega) = 94.2\sigma(\omega)$, where $\alpha(\omega)$ is in cm^{-1} and $\sigma(\omega)$ is in Ω^{-1} cm^{-1}. The dc resistivities at $T = 3$ K for samples 3, 4, 5, 6, and 7 are approximately 7×10^3, 320, 110, 80, and 20 Ω cm, respectively. Hence, the absorptions at zero frequency [i.e., $\alpha(0)$] are 0.01, 0.3, 0.9, 1.2, and 4.7 cm^{-1}. These values are consistent with those obtained from the extrapolated linear function fits shown in Fig. 5. This suggests that at low frequencies the absorption is approximately proportional to frequency.

The linear part of the absorption spectrum extends to higher frequencies as the impurity concentration increases. This linear frequency-dependent absorption at low frequencies is different from the Blinowski and Mycielski theory for n-type materials. The difference may be due to many reasons; for instance, at low frequencies, the absorption is theoretically predicted to be proportional to ωr_ω^3 [see Eq. (13)] where r_ω decreases as ω increases [see Eq. (5)] for the hydrogenlike model. The behavior of ωr_ω^3 is clearly different from the absorption which varies linearly with frequency, because of the term r_ω^3. However, if r_ω at low frequencies is less dependent on frequency than what is predicted by the hydrogenlike model, then the absorption will behave more linearly with frequency. Another possible explanation arises from the fact that the degree of compensation in NTD Ge is not small ($K > 0.2$). It can be shown that the Coulomb gap is of the order of the impurity band [12] and cannot be ignored in the low-energy regime. In this case the absorption at low frequencies should obey the expression in Eq. (14). The dependence of absorption on frequency is ω/r_ω; hence, the dependence on r_ω is weaker. It is noted that the dependence on r_ω is changed from r_ω^3 to $1/r_\omega$ due to the existence of the Coulomb gap. Although the linear frequency-dependent absorption is not clearly predicted from any theory, the possibility of having a weaker r_ω dependence is demonstrated. There are also dipole-dipole interactions which have been ignored in the above discussion, and which contribute a factor which depends logarithmically on the frequency.

The slope of these linear fitted lines at low frequencies ($d\alpha/d\omega|_{\text{low }\omega}$) versus carrier concentration is plotted in Fig. 4. The best fit curve to the power-law function for these data is obtained for the power $n = 1.0$. The theoretical slope of the absorption spectrum at $\omega = 0$ can be obtained from Eq. (13) and it is found to be proportional to $N_a^{4/3}$ (i.e., $n = \frac{4}{3}$). One of the factors contributing to this difference may be that the theoretical value is obtained for $T = 0$ K; whereas, the experimental value is obtained at $T = 3$ K. The nonzero temperature will have the largest effect on the absorption spectrum at low frequencies (i.e., $\hbar\omega < kT$).

The absorption of the samples at ω=30 cm^{-1} [$\alpha(30\ cm^{-1})$] is also plotted in Fig. 4, the best fit line being obtained for the power $n = 1.86$. In the high-frequency limit, it is theoretically found that the absorption is proportional to N_a^2 as in Eq. (15). The absorption in the region 22–32 cm^{-1} is found to vary almost linearly with frequency. The theory predicts that it is roughly proportional to r_ω^4.

Finally, the total absorption, which is defined as the area under the broad absorption for the hopping process, can be estimated from the spectra. The low-frequency absorption (< 4 cm^{-1}) is estimated by extending the linear fitted line of the spectrum. Similarly, the high-frequency absorption is estimated by extending the absorption curve in the linear region of the spectrum (22–32 cm^{-1}) to high frequencies. The results are plotted in Fig. 4. Sample 7 is not included in the best fit due to the large error which is caused by the strongly overlapping Ga impurity absorption. It is found that the best fit line is obtained for the power $n = 1.68$.

Figure 5 shows absorption spectra $V1$, $V2$, and $V3$ which were experimentally obtained by Vavilov *et al.*[7] for NTD Ge with different impurity concentrations. It is evident that their $V1$ and $V2$ absorption spectra are similar to the presented spectra samples 5 and 7 in the low-frequency region. Their $V1$ essentially overlaps sample 5 within the experimental uncertainty at frequencies below 10 cm^{-1} and $V2$ is only slightly below sample 7. The acceptor concentrations of $V1$ and $V2$ are 1.3 and 3×10^{16} cm^{-3}, respectively, which compare with 2.2 and 3.7×10^{16} cm^{-3} for samples 5 and 7, respectively. Thus, the present results are in good agreement with the results of Vavilov *et al.*, particularly at low frequencies. However, at high frequencies, a discrepancy exists between the two works. The absorption coefficient of samples 5 and 7 is higher than that of $V1$ and $V2$ for frequencies above 10 cm^{-1}.

Figure 6 shows the theoretical absorption spectra $T1$ and $T2$ found by Kaczmarek and Gortel[8] with N_a equal to 4.5 and 9×10^{15} cm^{-3}, respectively. The absorption coefficient per unit compensation, α/K, is plotted since the theoretical spectra are calculated with the assumption that $K < 0.2$ and in this case α/K is independent of K. Absorption spectra of samples 3 and 4 ($K = 0.286$) are shown for the purpose of comparison. It is first noticed that the theoretically predicted sharp peak is not observed. It is also found that the theoretical absorption curve $T2$ ($N_a = 9 \times 10^{15}$ cm^{-3}), is similar to sample 4 ($N_a = 14 \times 10^{15}$ cm^{-3}). Without considering the difference in N_a, the theoretical spectrum $T2$ is in excellent agreement with sample 4 for frequencies below 12 cm^{-1}. The theoretical absorption curve $T1$ ($N_a = 4.5 \times 10^{15}$ cm^{-3}), is close to, but below sample 3 ($N_a = 7 \times 10^{15}$ cm^{-3}). The general shape of these two spectra is similar for frequencies below 7 cm^{-1}. Considering that the the-

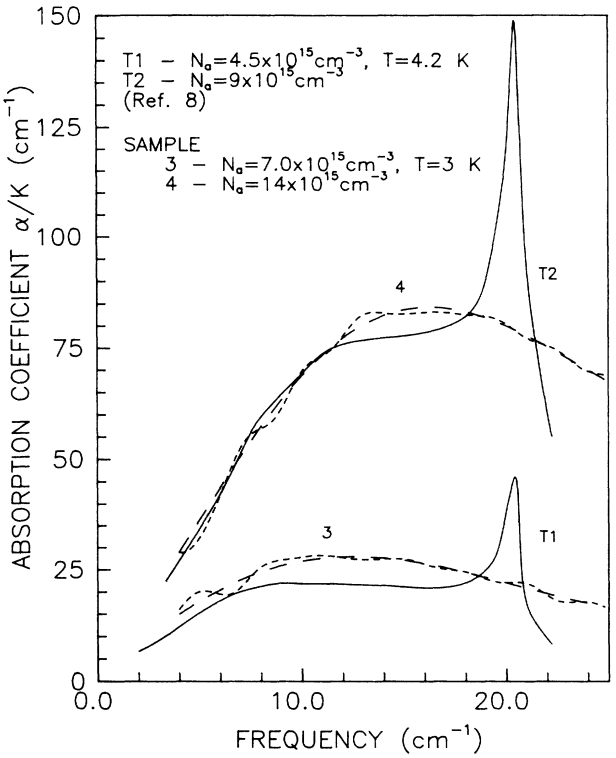

FIG. 6. The relative absorption coefficient α/K vs frequency for the theoretical spectra $T1$ and $T2$ obtained by Kaczmarek *et al.* for p-type Ge with $K < 0.2$ in the region from 2 to 22 cm^{-1}. The present results for samples 3 and 4 ($K = 0.286$) are shown together for comparison.

oretical curves ($T1$ and $T2$) do not have any adjustable parameters, these results show good agreement with the experimental spectra at low frequencies. However, when the concentration of acceptors N_a is taken into consideration, it is concluded that the magnitude of the predicted absorption is higher than the experimental value at low frequencies. The discrepancy may be due to two reasons: first, the function $F(\Omega, r)$ is not properly described by the much simplified form in Eqs. (9)–(12). As will be discussed below, the compensation ratio of the NTD Ge samples is 0.286, and therefore the Coulomb gap cannot be ignored. The number of states at low frequencies is limited by the existence of the Coulomb gap; therefore, $F(\Omega, r)$ in Eqs. (9)–(12) is overestimated in the low-frequency region. Second, the energy overlap integral is not as strong as that obtained by Kaczmarek *et al.*[8] using the Schechter envelope function.

As shown in Fig. 6, there is very little agreement between experiment and theory at higher frequencies. The theoretical curves predict that ω_{max} occurs at lower frequencies than that obtained experimentally. For instance, the maxima for $T1$ and $T2$ occur at about 8 and 11 cm^{-1}, compared to 12 and 16.3 cm^{-1} for samples 3 and 4. The theoretical spectra change very slowly with respect to frequency after these maxima below the frequency of the sharp peak that occurs at about 20 cm^{-1}. The absorption falls rapidly after this peak. None of these features are observed in the experimental spectra.

Kaczmarek *et al.*[8] have provided some comments on the possibility of the nonexistence of their predicted sharp peak. Firstly, the nonexistence of the sharp peak may be due to some factor not taken into account in the theory, such as angular dependence of the resonance energies, which may give rise to a peak which is much broader than predicted. Secondly, the Schechter functions are known to make the set of effective-mass equations internally inconsistent in an asymptotic limit as $r \rightarrow \infty$.[8] Therefore, it is possible that the Schechter envelope functions used in the theory do not properly describe the behavior of holes at intermediate distances from the impurity which are important in this theory.

Figure 7 shows the absorption spectrum of compensated n-type Si obtained by Milward *et al.*[2] in the region between 15 and 80 cm^{-1}. This sample has $N_d = 2.1 \times 10^{17}$ cm^{-3} and K=0.09. The absorption coefficient for the Si spectrum has been multiplied by 10. It is clear that the absorption coefficient for n-type Si is much weaker than that for NTD Ge. However, the general shape of the absorption spectra of the NTD Ge samples is very similar to that of the n-type Si sample. These results contradict the previous belief that the fre-

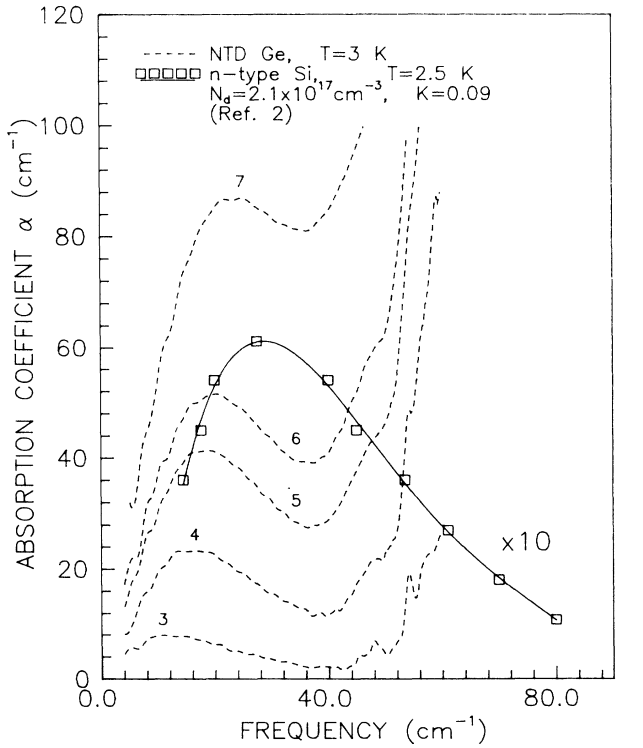

FIG. 7. Comparison of the present absorption spectra for NTD Ge samples to that of the n-type Si sample with $N_d = 2.1 \times 10^{17}$cm^{-3}, and $K = 0.09$ as obtained by Milward *et al.* Note that the absorption coefficient of the Si sample is enlarged by a factor of 10.

quency dependence of the absorption coefficient is less pronounced in p-type than in n-type materials. It is clear that at higher frequencies the shape of the NTD Ge spectra is closer to the n-type Si spectrum than to the theoretically predicted spectra shown in Fig. 6. It is also found (Fig. 4) that the general behavior of the broad absorption maxima of these p-type NTD Ge samples is similar to the theoretically predicted n-type Si spectra. This observation, together with the fact that there is no evidence for a sharp absorption peak, indicates that the presence of the d-like contributions in the Schechter envelope function are not as important as the theory predicted. The weaker contribution probably implies a smaller absorption coefficient. This is also consistent with the lower observed absorption than this theory predicts. The similar shape of the NTD Ge and n-type Si spectra beyond the maximum absorption may indicate that the form of interactions (the energy overlap integral and quantum effects, etc.) are similar at high frequencies. However, explaining the much higher absorption coefficient for p-type Ge may require more than simply using different parameters in the hydrogenlike envelope wave function to describe an acceptor. The correct order of magnitude of the absorption coefficients predicted by the theory of Kaczmarek *et al.*[8] indicates that the Schechter envelope wave function is a good starting point.

B. Time-dependent spectra for NTD Ge

This section presents the results of an investigation of the dynamical change of absorption due to the evolution of Ga impurities. This is accomplished by performing a series of time-dependent absorption experiments shortly after irradiation of a sample. Sample 5, which was irradiated for 10 h, was used for this experiment.

In order to monitor the change of the sample, an extra sample was prepared simultaneously with sample 5 so that it could be used concurrently for a resistivity measurement. This measurement was done using a four-point probe configuration[29] at room temperature. Figure 8 shows the change of resistivity with respect to time for this sample. Zero time is defined as the time when the irradiation began. It is clearly seen that the resistivity of the sample first increases, and then peaks at time $t_0 = 5.65$ d, followed by an asymptotic decrease to its steady-state value. As discussed in Sec. III, the donor concentration, N_d reaches its saturated value shortly after the irradiation, and the sample is n type for $t \leq t_{(K=1)}$. During this period of time, the Ga acceptor will act as a minority impurity and its increasing concentration N_a will effectively decrease the number of electron carriers which are mainly contributed by the donor. Therefore, the resistivity of the sample will increase as more Ga is created until it reaches a maximum resistivity at which $N_a \approx N_d$. Due to the difference in the mobilities of electrons and holes, the time for total compensation $t_{(K=1)}$ occurs at a slightly different time than the time for maximum resistivity t_0. However, the

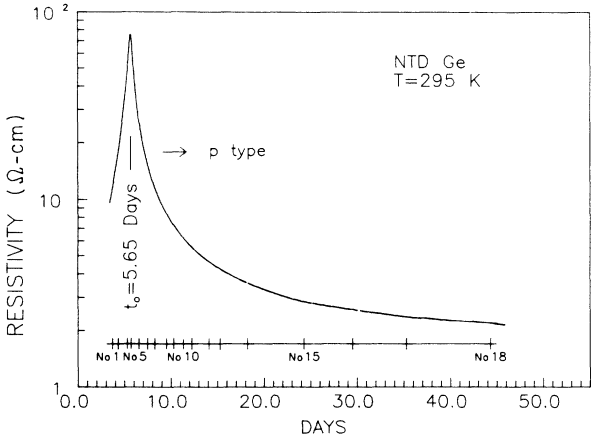

FIG. 8. The time-dependent resistivity for NTD Ge. Note that the total compensation ($K = N_a/N_d = 1$) occurs at time approximately $t_0 = 5.65$ d. The unit of the resistivity shown is not absolute.

difference between $t_{(K=1)}$ and t_0 is estimated to be less than 1% in this case. After $t_{(K=1)} \approx t_0$, the Ge sample becomes p type, and the resistivity starts to decrease because the number of hole carriers, due to the increasing Ga impurity increases.

Using the decay half-life of 11.2 d for Ga and $t_{(K=1)} \approx t_0 = 5.65$ d, the concentration of Ga at t_0 can be found from Eq. (21). The compensation ratio, which can be obtained approximately from $N_a(t_0)/N_a(t \rightarrow \infty)$ because $N_a(t_0) \approx N_a(t_{(K=1)}) \approx N_d(t \rightarrow \infty)$, is found to be 0.286. This is in good agreement with previous results.[25]

The series of absorption experiments are numbered in Fig. 8. Figure 9 shows the absorption spectra of exper-

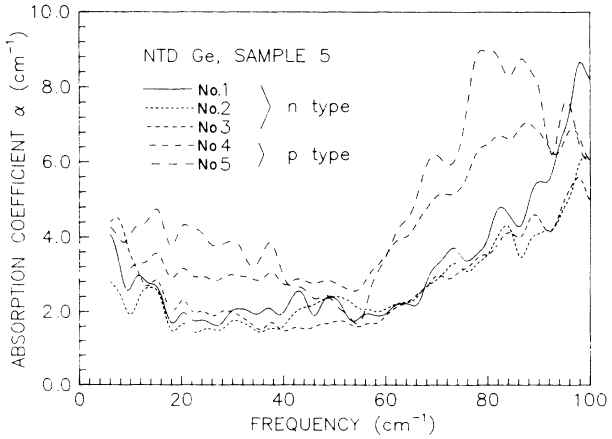

FIG. 9. Time-dependent absorption spectra for the NTD Ge sample 5. Spectra Nos. 1–5 are presented in the region 0–100 cm^{-1}. Note that there is a considerable difference between the n-type spectra (Nos. 1–3) and the p-type spectra (Nos. 4 and 5).

iment Nos. 1–5. The absorption spectra Nos. 1–3 are obtained at the times 3.7, 4.3, and 5.3 d. The sample is n type when these three measurements were made. The concentration of donors is 6.2×10^{15} cm^{-3} ($0.286N_a$), while the compensation, $K(t) = [N_a(t)/N_d]$, for these spectra is 0.68, 0.78, and 0.95 respectively. Spectra Nos. 4 and 5 are obtained at times 5.7 and 6.5 d, shortly after the sample is converted to a p-type material at day 5.65. The compensation, $K(t)$, for these two spectra is 0.99 and 0.89, respectively, with fixed N_d. It is clear that the far-infrared absorption for n-type Ge differs appreciably from that of p type. For instance, the absorption above 50 cm^{-1} is mainly due to the transition from the ground state to excited states of an impurity. It should be noticed that the absorption due to the As impurity in spectra Nos. 2 and 3 is small compared to No. 1. This is a result of the fact that more electrons are compensated by the increasing Ga concentration. When the sample turns p type, the absorption of the impurity, which will be due to the Ga impurity, starts at lower frequencies ($\approx$ 55 cm^{-1}). This difference can be explained by the different absorption spectra of Ga and As impurities in Ge.[34,37] The ionization energies for Ga and As are about 88.7 and 104.8 cm^{-1}, respectively.[29]

The absorption below 50 cm^{-1} is mainly due to photon-induced hopping of a charge carrier between impurity centers. In spectra Nos. 1–3, the absorption is weak in the region between 20 and 60 cm^{-1} and starts to increase towards lower frequencies. Therefore, it is concluded that absorption due to photon-induced hopping in n-type Ge occurs mainly for frequencies below 10 cm^{-1}. As the sample turns p type, the absorption suddenly increases for frequencies below 50 cm^{-1} and the maximum of a broad absorption starts to develop at a frequency above 10 cm^{-1}. This can be seen in Fig. 10. Compared to the p-type Ge absorption spectra, the absorption for n-type Ge is much weaker and occurs at lower frequencies.

Figure 10 shows absorption spectra Nos. 6–18 which were obtained during the period between day 7.5 and day 44.3. The compensation, $K(t)$ [$= N_d/N_a(t)$], varies from 0.79 to 0.31, respectively. This figure shows an increasing absorption coefficient for all frequencies in the region shown with respect to the time. The ω_{max} shifts from 15 to 18.3 cm^{-1} while $\alpha(\omega_{max})$ increases from 6.5 to 40 cm^{-1} during this post-irradiation period. These changes result from the increasing Ga impurity concentration.

A series of graphs shown in Fig. 11 illustrate the changes in the absorption properties with respect to the time. The plotted data shown in this figure is obtained only after the broad absorption peaks of spectra Nos. 6–18 are fit to a polynomial function. These changes in the absorption properties are due to the time evolution of Ga in the sample. That is, the changes correspond to the change of the majority impurity concentration, N_a, for a fixed minority concentration. To see how the absorption properties change with respect to N_a, these results are treated in a manner similar to those in the previ-

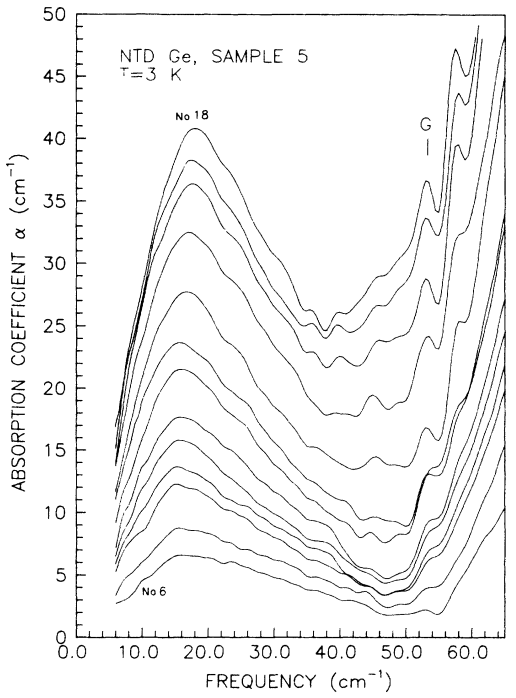

FIG. 10. Time-dependent spectra of NTD Ge. The spectra Nos. 6–18 are presented in the region from 6 to 65 cm^{-1}.

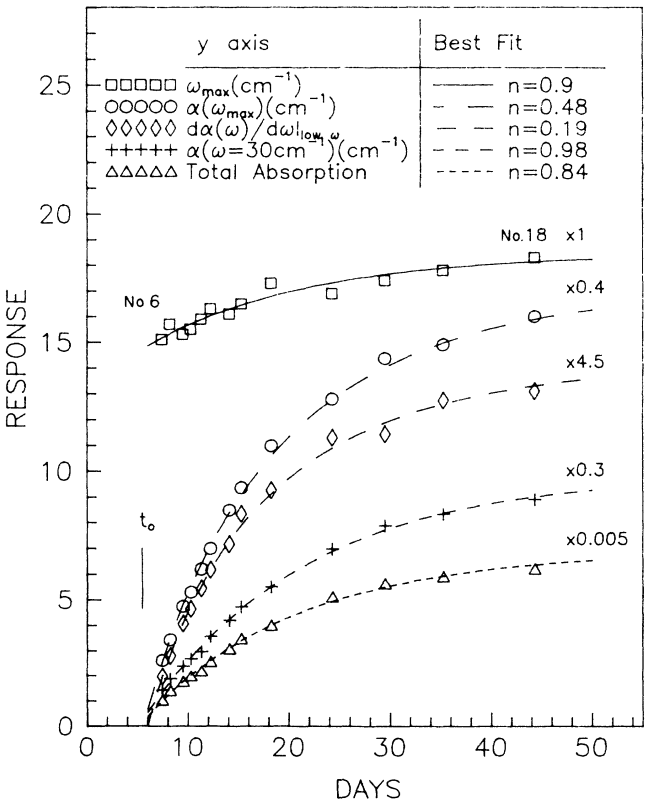

FIG. 11. General properties of the absorption spectra in Fig. 10 vs time. Data are least-squares fit with the function $y = a(N_a)^n + b$. The time at which the sample is totally compensated is indicated by t_0.

ous section, whereby the various data are least-squares fit to the power-law function $y = a(N_a)^n + b$, where N_a is first obtained using Eq. (21) with a half-life of 11.2 d. It is found that the power dependence on N_a of ω_{max}, $\alpha(\omega_{max})$, $d\alpha/d\omega|_{low\ \omega}$, $\alpha(30\ cm^{-1})$ and the total absorption is 0.9, 0.48, 0.19, 0.98, and 0.84, respectively.

The differences between the absorption characteristics of samples with different impurity concentrations, but with the same compensation and those with different majority impurity concentrations, but with fixed minority impurity concentration are shown in Table V. The $\alpha(\omega_{max})$, $d\alpha/d\omega|_{low\ \omega}$, $\alpha(30\ cm^{-1})$, and the total absorption are all related to the absorption coefficient of the sample. The power factor of these properties on impurity concentration in samples with different concentration but fixed compensation is higher than that of the samples with fixed N_d and varied N_a. The differences are 0.83, 0.81, 0.88, and 0.84, respectively. All of these differences involve a factor close to one. According to the Blinowski and Mycielski theory, the absorption is proportional to the concentration of the minority impurity for $K < 0.2$. Therefore, the difference between the values of the power, n, needed to fit the data describing $\alpha(\omega_{max})$ of the broad absorption should be one because in one case N_d is fixed and for the other case N_d varies as KN_a. The present experimental value is 0.83. Similarly, if $f(K)$, in Eq. (13), is independent of K, then a difference of one in the value of n should also be obtained for the dependence of the slope of the spectra as $\omega \rightarrow 0$ and for the absorption at high frequencies. [see Eq. (15)]. The present results are 0.81 for $d\alpha/d\omega|_{low\ \omega}$ and 0.88 (evaluated at 30 cm^{-1}) respectively. It is clear that the assumption that the function $F(\Omega, r)$depends only linearly on the minority impurity concentration and that $f(K)$ is independent of K cannot hold for the time-dependent absorption spectra because K is always larger than 0.286. Thus, the present results support the theory based on the localized-pair model.

According to Eq. (16), the frequency at which the maximum of the absorption, ω_{max}, occurs depends only on the majority impurity concentration. This implies that the dependence of N_a on the maximum should be the same for these two types of absorption spectra. However, there is large uncertainty involved in the results for the time-dependent spectra as shown in Fig. 11. For instance, the best fit line with $n = 0.9$ is not much better than a fit with $n = 0.37$. No conclusion can be made for the frequency of the absorption maximum from these results.

V. CONCLUSIONS

Far-infrared absorption of photon-induced hopping in compensated p-type NTD Ge at 3 K has been presented. Based on the results of the absorption spectra, it is concluded that the overall behavior is consistent with the theory based on the localized model.[1] For instance, (i) the absorption coefficient increases with increasing impurity concentration, and (ii) there exists a broad absorption peak whose maximum shifts to higher frequencies as the majority impurity increases.

A power-law function fit was used to characterize the general behavior of the experimental spectra due to a change in the majority impurity concentration. The values of the powers derived from the experimental spectra, in general, agree with those obtained from theory. For example, the experimental results derived from samples with different impurity concentrations, but with fixed compensation show that the ω_{max} and $\alpha(\omega_{max})$ of the broad absorption maxima varies with the majority impurity concentration as $N_a^{0.37}$ and $N_a^{1.31}$, respectively. These values are close to the values $N_d^{0.41}$ and $N_d^{1.36}$ obtained from the numerical calculation for n-type Si spectra based on the Blinowski and Mycielski theory. The slope of the low-frequency spectra varies as $N_a^{1.0}$ at $T = 3$ K which is to be compared with the theoretical result $N_a^{4/3}$ obtained at zero frequency and $T = 0$ K. Also, the absorption at 30 cm^{-1} varies as $N_a^{1.86}$ which is compared to the theoretical result of N_a^2 at high frequencies.

Similarly, the results derived from the time-dependent absorption experiments can be fit to the power-law function. The time-dependent Ga concentration is calculated from the known decay process. In this case, the absorption spectrum changes due to the increasing majority impurity (Ga) concentration (N_a). Comparing the power dependence on N_a of $\alpha(\omega_{max})$, $d\alpha/d\omega|_{low\ \omega}$, $\alpha(30\ cm^{-1})$, and the total absorption to the fixed compensation case, shows that these dependences on N_a are approximately smaller by a power of one. This indicates that the absorption coefficient is almost directly proportional to the concentration of minority impurities because N_d $(= KN_a)$ is fixed in this case. Once again, this conclusion agrees with the Blinowski and Mycielski theory based on the localized-pair model [see $F(\Omega, r)$ in Eqs. (9)–(12)]. It is interesting to note that the power-law functions are fit to the time-dependent absorption spectra whose compensation ratio varies from $K = 0.8$ to 0.3. The function $F(\Omega, r)$ in this case is no longer simply proportional to

TABLE V. Properties of absorption spectra for NTD Ge.

N_a^n	ω_{max}	$\alpha(\omega_{max})$	$d\alpha/d\omega\|_{low\omega}$	$\alpha(30\ cm^{-1})$	Total absorption
n (K =fixed)	0.37	1.31	1.00	1.86	1.68
n (N_d=fixed)	0.90	0.48	0.19	0.98	0.84
Difference	−0.53	0.83	0.81	0.88	0.84

the minority impurity concentration because $K > 0.2$. This may explain, in part, why the differences in the power n are consistently smaller than one for those properties related to the absorption as shown in Table V.

The present spectra are in agreement with previous NTD Ge absorption experiments performed by Vavilov *et al.*[7] for frequencies below 10 cm^{-1}. However, at high frequencies, a discrepancy exists between the two works. The absorption coefficient of the present spectra is higher than that of Vavilov *et al.* for frequencies above 10 cm^{-1}. A comparison of these results with the theory of Kaczmarek *et al.*[8] for p-type materials shows reasonable agreement at low frequencies but even at these frequencies the predicted absorption coefficient is somewhat too high. At high frequencies, there are several discrepancies between their theory and the present results. The general shapes of the spectra are different; specifically, the predicted sharp peak is not observed.

Hence, the present work certainly confirms the previous conclusions[8] that the absorption coefficient for p-type Ge is much higher and that its maximum occurs at higher frequencies than that of n-type Ge. However, this work cannot agree with the previous belief that the dependence of the absorption coefficient on frequency is less pronounced for p-type than for n-type Ge. In fact, when the present p-type Ge absorption spectra are compared with the n-type Si spectrum obtained by Milward *et al.*,[2] it is concluded that the general shape of the spectra is quite similar although n-type Si has a much weaker absorption and the absorption is at higher frequencies. It is speculated that in the high-frequency region, the interactions between p-type and n-type impurities are very similar. It is noted that in this region the theory for p-type materials based on the Schechter function does not agree with the experimental results. Similarly, it is found that the theory for n-type materials based on the hydrogenlike function does not agree well with the experimental results.[17] The discrepancies in both cases between theoretical and experimental results may have the same origin: the fact that quantum effects cannot be ignored in the high-frequency region. Quantum effects may also play a common role in both n- and p-type absorptions at high frequencies.

A linear function is fit to the low-frequency region of the spectrum. The absorption coefficient at $\omega = 0$ is extrapolated from the linear fit. It is found that this value is consistent with the value obtained from the dc resistivity measurement. It is concluded that the absorption is approximately proportional to frequency in the low-frequency region. This simple linear relationship between the absorption coefficient and the frequency is quite surprising. Some possible explanations are pointed out. (i) The dependence of r_ω on frequency is weak at low frequencies, and (ii) this linear behavior may be due to the existence of the Coulomb gap which limits the density of states at low energies.

It is clear that the understanding of the interactions in disordered systems is still far from complete. Far-infrared absorption experiments can certainly contribute to the understanding of certain aspects of such complex systems. Based on the results of this research, it is clear that some work on describing the interactions between acceptors is needed although the Schechter envelope function is certainly a good starting point. Further theoretical investigations are needed to include the quantum effects which are important at high frequencies. Further absorption experiments for frequencies below 5 cm^{-1}, which is the low-frequency limit of the present work, would be useful to confirm the proposed linear relationship. If this simple linear relationship is confirmed, then its understanding may provide some insight into the fundamental nature of these systems.

ACKNOWLEDGMENTS

We would like to thank Dr. A. A. Berezin for helpful discussions. We also thank J. D. Evans for the use of the Hall-measurement setup.

*Present address: Department of Engineering Physics, McMaster University, Hamiton, Ontario, Canada L8S 4M1.

[1] J. Blinowski and J. Mycielski, Phys. Rev. **136**, A266 (1964); J. Blinowski and J. Mycielski, Phys. Rev. **140**, A1024 (1965).

[2] R. C. Milward and L. J. Neuringer, Phys. Rev. Lett. **15**, 664 (1965); L. J. Neuringer, R. C. Milward, and R. L. Aggarval, J. Phys. Soc. Jpn. Suppl. **21**, 582 (1966).

[3] A. I. Demeshina, R. L. Korchazhkina, N. N. Kuznetsova, and V. N. Murzin, Fiz. Tekh. Poluprovodn. **4**, 428 (1970) [Sov. Phys.—Semicond. **4**, 363 (1970)].

[4] R. A. Smith, S. Zwerdling, S. N. Dermatis, and J. P. Theriault, in *Proceedings of the Ninth International Conference on the Physics of Semiconductors, Moscow, 1968,* edited by S. M. Ryvkin and Yu. V. Shmartsev (Nauka, Leningrad, 1968), p. 149.

[5] S. Zwerdling and J. P. Theriault, Infrared Phys. **12**, 165 (1972).

[6] Y. Nakagawa and H. Yoshinaga, J. Phys. Soc. Jpn **30**, 1212 (1972).

[7] V. S. Vavilov, A. G. Kazanskii, O. G. Koshelev and P. V. Reznikov, Fiz. Tekh. Poluprovodn. **10**, 1591 (1976) [Sov. Phys.—Semicond. **10**, 947 (1976)].

[8] E. Kaczmarek and Z. W. Gortel, Phys. Rev. B **10**, 2535 (1974).

[9] *Neutron Transmutation Doping in Semiconductors*, edited by J. Meese (Plenum, New York, 1979).

[10] E. E. Haller, N. P. Palaio, and M. Rodder, in *Neutron Transmutation Doping of Semiconductor Materials*, edited by R. D. Larrabee (Plenum, New York, 1982).

[11] Sir Nevill Mott, *Metal-Insulator Transitions* (Barnes and Nobles, New York, 1974).

[12]B. I. Shklovskii and A. L. Efros, *Electronic Properties of Doped Semiconductors* (Springer-Verlag, New York, 1984).
[13]M. Banaszkiewicz, Phys. Status. Solidi B **69**, 247 (1975).
[14]S. D. Baranovskii and A. A. Uzakov, Fiz. Tekh. Poluprovodn. **16**, 1606 (1982) [Sov. Phys.—Semicond. **16**, 1026 (1982)].
[15]S. Tanaka and H. Y. Fan, Phys. Rev. **132**, 1516 (1963).
[16]A. Miller and E. Abrahams, Phys. Rev. **120**, 745 (1960).
[17]A. L. Efros and B. I. Shklovskii, in *Electron-Electron Interactions in Disordered Systems*, edited by A. L. Efros and M. Pollak (North-Holland, Amsterdam, 1985).
[18]S. D. Baranovskii and A. A. Uzakov, Fiz. Tekh. Poluprovodn. **15**, 931 (1981) [Sov. Phys.—Semicond. **15**, 533 (1981)].
[19]A. L. Efros and B. I. Shklovskii, J. Phys. C **8**, L49 (1975).
[20]B. I. Shklovskii and A. L. Efros, Zh. Eksp. Teor. Fiz. **81**, 406 (1981) [Sov. Phys.—JETP **54**, 218 (1981)].
[21]J. H. Davies, P. A. Lee, and T. M. Rice, Phys. Rev. B **29**, 4260 (1984).
[22]D. Schechter, J. Phys. Chem. Solids **23**, 237 (1962).
[23]E. Kaczmarek, Acta Phys. Polon. **30**, 267 (1966); **30**, 277 (1966); **30**, 283 (1966).
[24]Z. W. Gortel and E. Kaczmarek, Acta Phys. Polon. A **41**, 641 (1972).
[25]Y. A. Osip'yan, V. M. Prokopenko, and V. I. Tal'yanskii, Zh. Eksp. Teor. Fiz. **87**, 269 (1984) [Sov. Phys.—JETP **60**, 156 (1984)].
[26]K. Kuriyama, M. Yahagi, and K. Iwamura, J. Appl. Phys. **54**, 673 (1983).
[27]G. Cripps, M.Sc. thesis, McMaster University, 1986 (unpublished).
[28]L. J. Van der Pauw, Philips Res. Rep. **13**, 1 (1958).
[29]S. M. Sze, *Physics of Semiconductor Devices* (Wiley, New York, 1981).
[30]F. J. Morin, Phys. Rev. **93**, 62 (1954).
[31]I. S. Park and E. E. Haller, J. App. Phys. **64**, 6775 (1988).
[32]C. M. Randall and R. D. Rawcliffe, Appl. Opt. **6**, 1889 (1967).
[33]R. J. Bell, *Introductory Fourier Transform Spectroscopy* (Academic, New York, 1972).
[34]R. L. Jones and P. Fisher, J. Phys. Chem. Solids **26**, 3125 (1965).
[35]G. A. Thomas, M. Capizzi, F. DeRosa, R. N. Bhatt, and T. M. Rice, Phys. Rev. B **23**, 5472 (1981).
[36]F. W. Wooten, *Optical Properties of Solids* (Academic, New York, 1972).
[37]P. Fisher and A. K. Ramdas, in *Physics of the Solid State*, edited by S. Balakrishna, M. Krishnamurti, and B. Ramachandra (Academic, London, 1969).